ISSN 1063-7834, Physics of the Solid State, 2015, Vol. 57, No. 10, pp. 1921–1931. © Pleiades Publishing, Ltd., 2015.
Original Russian Text © T.I. Spiridonova, A.V. Bakulin, S.E. Kulkova, 2015, published in Fizika Tverdogo Tela, 2015, Vol. 57, No. 10, pp. 1873–1882.

METALS

Interaction of Hydrogen with Impurities in Group IVB Metals

T. I. Spiridonova[a], A. V. Bakulin[b, c], and S. E. Kulkova[b, c, *]

[a] *National Research Tomsk Polytechnic University, pr. Lenina 30, Tomsk, 634050 Russia*
[b] *Institute of Strength Physics and Materials Science, Siberian Branch of the Russian Academy of Sciences, pr. Akademicheskii 2/4, Tomsk, 634055 Russia*
* *e-mail: kulkova@ispms.tsc.ru*
[c] *National Research Tomsk State University, pr. Lenina 36, Tomsk, 634050 Russia*

Received March 5, 2015

Abstract—The energetics of hydrogen bonding with Group IVB metals and the interaction of hydrogen with impurities of 3*d*-transition and simple metals (Al, Ga, Si, Ge) have been investigated using the projector-augmented-wave (PAW) method within the framework of the density functional theory (DFT). It has been found that the solubility of hydrogen in Ti, Zr, and Hf increases upon their alloying with metals located in the middle of the 3*d* period. The relationship between the interaction energy of hydrogen with impurities, the lattice distortions, and the electronic structure of the studied systems has been analyzed. It has been shown that impurities do not affect the preferred hydrogen sorption positions in titanium but can change these positions in zirconium and hafnium. The influence of impurities and hydrogen on the electronic structure of metals has been examined. The obtained results have demonstrated that, in the studied metals, the interactions of hydrogen with impurities of 3*d*-transition and simple metals are determined by different mechanisms: the attraction of hydrogen by transition metal impurities is caused by the size effect, whereas the repulsion of hydrogen by simple metals can be associated with the electronic factors.

DOI: 10.1134/S1063783415100315

1. INTRODUCTION

It is known that Group IVB metals (titanium, zirconium, and hafnium) have been widely used for various technological applications. Titanium has the best strength-to-weight ratio and high corrosion resistance. Consequently, this metal has been widely used in the aerospace and automotive industries, as well as in medicine. Zirconium, hafnium, and their alloys have been actively used in the atomic industry and nuclear power engineering. The presence of hydrogen in Group IVB metals and their alloys is one of the factors responsible for the degradation of these materials during operation. Since these metals have a good affinity to hydrogen, they are characterized by a high capacity for its absorption. Their hydride phases are quite easily formed, which leads to a significant deterioration of the mechanical properties [1, 2]. The hydrides formed based on Group IVB metals exhibit a set of interesting physical properties, and their phase transformations differ from those observed in these metals [3]. The electronic structure and physicochemical properties of both pure Group IVB metals and their hydrides have been intensively investigated using theoretical methods [4–15]. Although hydrogen in metals has been studied since the beginning of the last century [1, 2], some aspects of its interaction with metals are still not clearly understood. In a number of studies [16–21], it was shown that the solubility of hydrogen in transition metals can be increased by their alloying, which is associated with the trapping of hydrogen by impurity atoms. At the same time, there are contradictory experimental data on the influence of impurities of simple metals on the solubility of hydrogen in metals [17, 18]. A detailed theoretical investigation of the influence of impurities of simple and transition metals on the solubility of hydrogen in titanium was performed by Hu et al. [14] using the linear muffin-tin (MT) orbital method (LMTO) [22]. These authors concluded that simple metals repel hydrogen, whereas transition metal atoms with smaller ionic radii than those of the matrix atoms attract hydrogen. It was also shown that hydrogen prefers to occupy tetrahedral (*T*) positions in titanium. The difference in the total energies for the systems with hydrogen in the tetrahedral and octahedral (*O*) positions is equal to ~2.0 eV. At the same time, in other theoretical studies, for example, in [13, 15], the octahedral configuration for hydrogen was found to be more preferable than the *T* position.

It is known that, in the literature, the preferred position of hydrogen in Group IV metals remains controversial. Hempelmann et al. [23] performed a comparison of the experimental results for Group IVB metals with the previously obtained data for dihydrides and came to the conclusion that hydrogen predominantly occupies octahedral positions in α-Ti and tetrahedral positions in zirconium. At the same time, for titanium at approximately the same temperature as in

Table 1. Lattice parameters of Group IV metals in the hexagonal structure

Metal	Ti	Zr	Hf
a, Å	2.921	3.237	3.192
c/a, Å	1.586	1.595	1.581
a, experiment [34]	2.945	3.23	3.20
c/a, experiment [34]	1.588	1.593	1.582

[23], Khoda-Bakhsh and Ross [24] revealed only a single peak, which was attributed by these authors to hydrogen in tetrahedral positions. It should be noted that, in the theoretical studies [25–27] performed by different methods, it was also shown that hydrogen prefers to occupy octahedral positions, and the difference between the energies in this case lies in the range from 0.076 to 0.520 eV.

The purpose of this work was to perform a comparative study of the hydrogen absorption in Group IVB metals and the mechanisms of interaction of hydrogen with substitutional impurities of simple and transition metals.

2. COMPUTATIONAL METHOD

The electronic structure of Group IVB metals in the hexagonal phase was calculated using the projector-augmented-wave (PAW) method [28, 29] implemented in the VASP computer code [30, 31] with the generalized gradient approximation proposed by Perdew, Burke, and Ernzerhof for the exchange-correlation functional (GGA-PBE) [32]. The cutoff energy for plane waves was 600 eV. The convergence in the total energy was considered to be achieved when the difference between the total energies for two successive iterations did not exceed 10^{-5} eV. The integration over the Brillouin zone was performed on a Γ-centered $9 \times 9 \times 9$ k-point mesh [33]. The atomic positions were relaxed until the forces of no more than 0.01 eV/Å at the atoms were achieved.

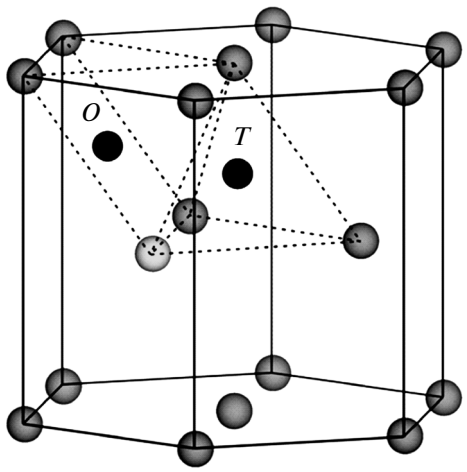

Fig. 1. Octahedral (O) and tetrahedral (T) positions of hydrogen in the hexagonal lattice of Group IVB metals. Gray and white balls indicate metal atoms and impurity atoms, respectively.

In the calculations, we used a $2 \times 2 \times 1$ supercell that, as in [14], contained eight titanium atoms, one of which was later replaced by an impurity atom. It is known that the computational cell can be optimized by several methods. In this regard, it was interesting to compare the results obtained after the optimization of the cell volume with the results of the calculations that included the relaxation of atomic positions with retaining the shape of the crystal. In the latter case, the procedure of optimizing the cell volume and atomic positions was repeated several times until the necessary criteria for the convergence were achieved. In addition, the optimization was performed both for the unit cells containing two metal atoms and for the enlarged cells. Along with the relaxation of atomic positions, this optimization included the change in the shape of the crystal. The theoretical lattice parameters calculated for metals in the latter case were in good agreement with the experimental data (Table 1). The octahedral position of hydrogen had the coordinates (2/3, 1/3, 1/4), and the initial coordinates for hydrogen in the T position were the same as in [14]: (5/6, 1/6, z_T), where $z_T = a^2/(12c^2)$. The impurity atom occupied the position closest to the hydrogen atom, as is shown in Fig. 1.

The binding energy of hydrogen in the metal matrix was calculated according to the formula

$$E_b = E(N, X, I) - E(N, X) - E(I), \quad (1)$$

where N is the number of positions in the supercell, X is the substitutional impurity, I is the interstitial impurity, $E(N, X)$ is the total energy of the system with the substitutional impurity, $E(N, X, H)$ is the total energy of the system with the substitutional and interstitial impurities, and $E(I)$ is the total energy of an isolated atom of the interstitial impurity. The absorption energy was calculated using the formula similar to expression (1). In this case, instead of the energy of the hydrogen atom, we calculated half of the total energy of the hydrogen molecule. Thus, the absorption energy of hydrogen in metals differs from the binding energy of hydrogen by half of the binding energy of hydrogen atoms in the H_2 molecule.

The interaction energy of hydrogen with an impurity atom was calculated according to the formula

$$\Delta E = [E(N, X, I) + E(N)] - [E(N, X) + E(N, I)], \quad (2)$$

where $E(N)$ is the total energy of the cell with atoms of the studied metal.

Table 2. Binding energies E_b and absorption energies E_{abs} of hydrogen atoms located at different positions in Group IVB metals according to the data obtained after the optimization of the cell volume and after the additional relaxation of the atomic positions (in parentheses)

Metals	E_b, eV		E_{abs}, eV	
	O position	*T* position	*O* position	*T* position
Ti	−2.65 (−2.71)	−2.42 (−2.55)	−0.38 (−0.44)	−0.15 (−0.28)
Zr	−2.64 (−2.67)	−2.59 (−2.67)	−0.37 (−0.40)	−0.32 (−0.40)
Hf	−2.51 (−2.56)	−2.51 (−2.60)	−0.24 (−0.29)	−0.24 (−0.33)

The relative change in the cell volume of a Group IVB metal upon doping with different metals was estimated from the formula

$$\Delta V(N, X) = \frac{V(N, X) - V(N)}{V(N)}, \quad (3)$$

where $V(N, X)$ is the volume of the cell containing the substitutional impurity and $V(N)$ is the cell volume of the metal matrix. The relative increase in the cell volume upon hydrogen sorption was calculated according to a similar formula.

3. RESULTS AND DISCUSSION

3.1. Binding and Absorption Energies of Hydrogen in Group IVB Metals

Table 2 presents the binding and absorption energies of hydrogen atoms in the metal matrix according to the calculations for the $2 \times 2 \times 1$ cell. It can be seen that the binding energy of hydrogen atoms in the octahedral positions is greater in magnitude than that in the tetrahedral positions. Recall that the higher absolute value of the binding energy means a stronger bond in the metal matrix. In the case of zirconium, the binding energies of hydrogen in the two positions are almost equal to each other, whereas in hafnium, the sorption of hydrogen in tetrahedral positions is preferable. It should be noted that, in the second optimization model, the ratio c/a is equal to the experimental value and does not change during the relaxation. For titanium, the difference in the binding energies of hydrogen in the *O* and *T* positions is equal to ~0.15 eV. This value is in the range of values obtained in earlier works: it is larger than the value obtained in [26] but is smaller than the value calculated in [27]. It can be seen from Table 2 that, in Group IV metals, the binding and absorption energies of hydrogen in two positions, respectively, are very close to each other. The inclusion of the zero-point vibrational energies of hydrogen atoms in the molecule and in the metal does not affect the revealed trends. In this case, the corrections of 0.12 and 0.03 eV for hydrogen atoms in the *T* and *O* positions in titanium are in good agreement with the results obtained using the PAW–GGA method in [13].

Let us consider the results obtained in the experimental studies [23, 24, 35]. In [35], it was shown that hydrogen in ZrH_2 contributes to the vibrational spectrum at an energy of 137 meV. In [23], it was found that the vibrational spectrum of α-Zr exhibits a peak at an energy of 143.1 meV. Since hydrogen in zirconium dihydride occupies tetrapores, the authors of [23] concluded that, in pure zirconium, hydrogen is also embedded in the *T* positions. A more complex situation is observed in titanium, because the vibrational spectrum of α-Ti at a temperature of 326°C contains a broad double peak with maxima at energies of 105.5 and 162.0 meV [23]. Since, for the mixed (α + δ) phase, there is only a single narrow peak at an energy of 150.5 meV, which can be attributed to hydrogen in the *T* position, the authors of [23] assumed that a greater part of the hydrogen atoms occupy the octahedral positions. In this context, the results of the present study on the hydrogen sorption in titanium agree with the experiment [23]. At the same time, in [24], it was found that, at approximately the same temperature (315°C), the vibrational spectrum of titanium contains only one peak at an energy of 141 meV, and an increase in the temperature to 715°C leads to the appearance of a broader peak with maxima at energies of 120, 141, and 171 meV, one of which at an energy of 141 meV was attributed to the *T* position, while the other two peaks were assigned to the vibrations of hydrogen atoms in a distorted *T* position in titanium with a body-centered cubic (bcc) phase. These conclusions were drawn based on the comparison with the results obtained for palladium with optical modes at energies of 68.5 meV [36], which was attributed to hydrogen in octapores. Reasoning from the evaluation of bond lengths, the authors of [24] assumed that, in the case of titanium, the vibrational modes of hydrogen in octapores should be at lower energies as compared to palladium. It should be noted that the situation with hydrogen in palladium is still a matter of debate [37]. In the theoretical study [13], the results obtained in [24] were reinterpreted and assigned to vibrations of hydrogen atoms in both positions.

It should be noted that another well-known interstitial impurity, namely, helium, prefers to occupy tetrahedral positions in zirconium, as was shown in [38], and the difference between the binding energies in the two positions is ~0.11 eV. In [38], the calculations were carried out using the linear augmented-plane-wave method implemented in the FLEUR code [39].

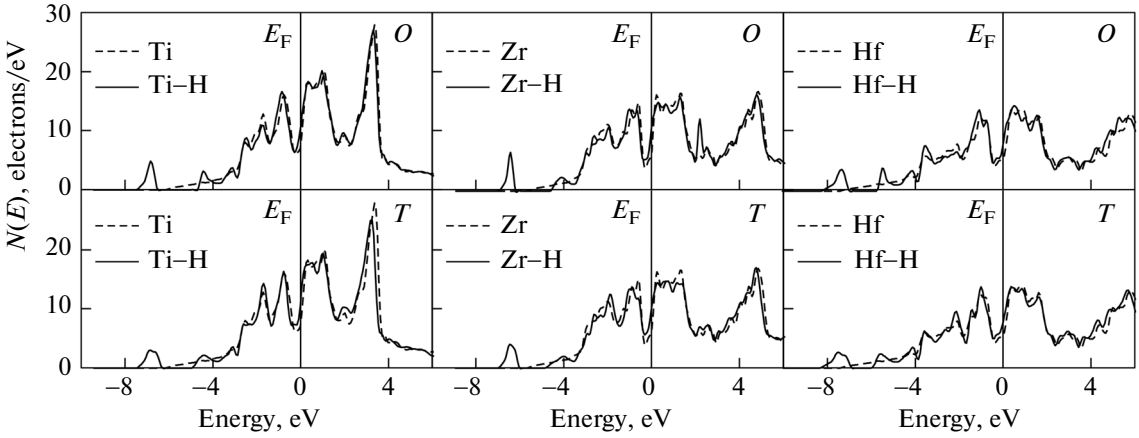

Fig. 2. Total densities of states of Group IVB metals with hydrogen in the *O* positions (upper panels) and the *T* positions (lower panels) in comparison with the densities of states in pure metals.

Almost the same binding energies of helium in zirconium (3.14 and 3.04 eV) for the *O* and *T* positions, respectively, were obtained using the PAW–PBE method in our work after the optimization of only the cell volume, and significantly lower values of 2.70 and 2.33 eV for the *O* and *T* positions, respectively, were obtained taking into account the optimization of the atomic positions. In the authors' opinion [40], since helium is an inert gas with a filled electron shell, it can mechanically more easily penetrate between four atoms into the *T* position than into the *O* position surrounded by six atoms. This conclusion is confirmed by our calculations of the mechanical contribution to the binding energy, which almost completely determines this energy and can be calculated as the difference between the energy of the system, from which the interstitial impurity atom was removed after the relaxation, and the energy of the equilibrium lattice of pure metal. In the case of hydrogen in titanium, the mechanical contribution to the binding energy, according to our calculations, is small enough and equal to 0.06 eV for the *O* position and 0.09 eV for the *T* position. The values of the same order of magnitude were obtained for other Group IV metals. Thus, the main contribution to the interaction of hydrogen with the metal matrix is a chemical contribution. Details of the calculations associated with the determination of different contributions to the energetics of the bonding of interstitial impurities in the metal matrix were described in [41]. For the formation of a strong bond, the more energetically favorable position of hydrogen is located closer to the metal.

The estimation of the pore radii for the incorporation of hydrogen into Group IV metals demonstrates that the octapore radius R_O is equal to 0.75–0.82 Å, whereas the tetrapore radius R_T varies in the range from 0.45 to 0.51 Å. According to the theoretical data [13], hydrogen accepts approximately 0.7–0.8 electron from titanium atoms. Recall that the covalent and ionic radii of hydrogen are equal to 0.32 and 0.54 Å, respectively. It is obvious that, structurally, hydrogen is more easily embedded in the *O* position.

The length of the hydrogen bond with titanium in TiH_2 is estimated as 1.91 Å, whereas the distances from the centers of the tetrapore and octapore are equal to 1.79 and 2.07 Å, respectively. This also indicates that hydrogen atoms are difficult to occupy the *T* positions in titanium, but the incorporation of hydrogen atoms into these positions in zirconium and hafnium occurs more easily, because their volume increases by more than 30%. Since the introduction of hydrogen into any position in the metal leads to an expansion of the lattice, the subsequent sorption into the *T* position becomes easier. An increase in the temperature results in an expansion of the crystal, which also favors the incorporation of hydrogen into the tetrapore.

In conclusion, we emphasize that the difference in the binding energies of hydrogen in the *O* and *T* positions decreases from 0.15 to 0.03 eV, when the calculation is performed for the titanium cell volume increased by 10%. Since the direct determination of the hydrogen positions in materials from the experiment is complicated, in the first-principles calculations the procedure of optimizing the computational cell and the use of the approximation for the exchange-correlation functional are of fundamental importance.

The total electron densities of states of the studied metals with hydrogen in two sorption positions are shown in Fig. 2. It can be seen that, in pure metals, the Fermi level lies in the valley between two density-of-states peaks, which is consistent with earlier calculations [6–8]. Regardless of the hydrogen sorption position, the density-of-states curves for all metals near the bottom of the valence band of the metal demonstrate a split-off band located at an energy of approximately –7 eV. The appearance of these small density-of-states peaks is caused by the interaction of the *s* and

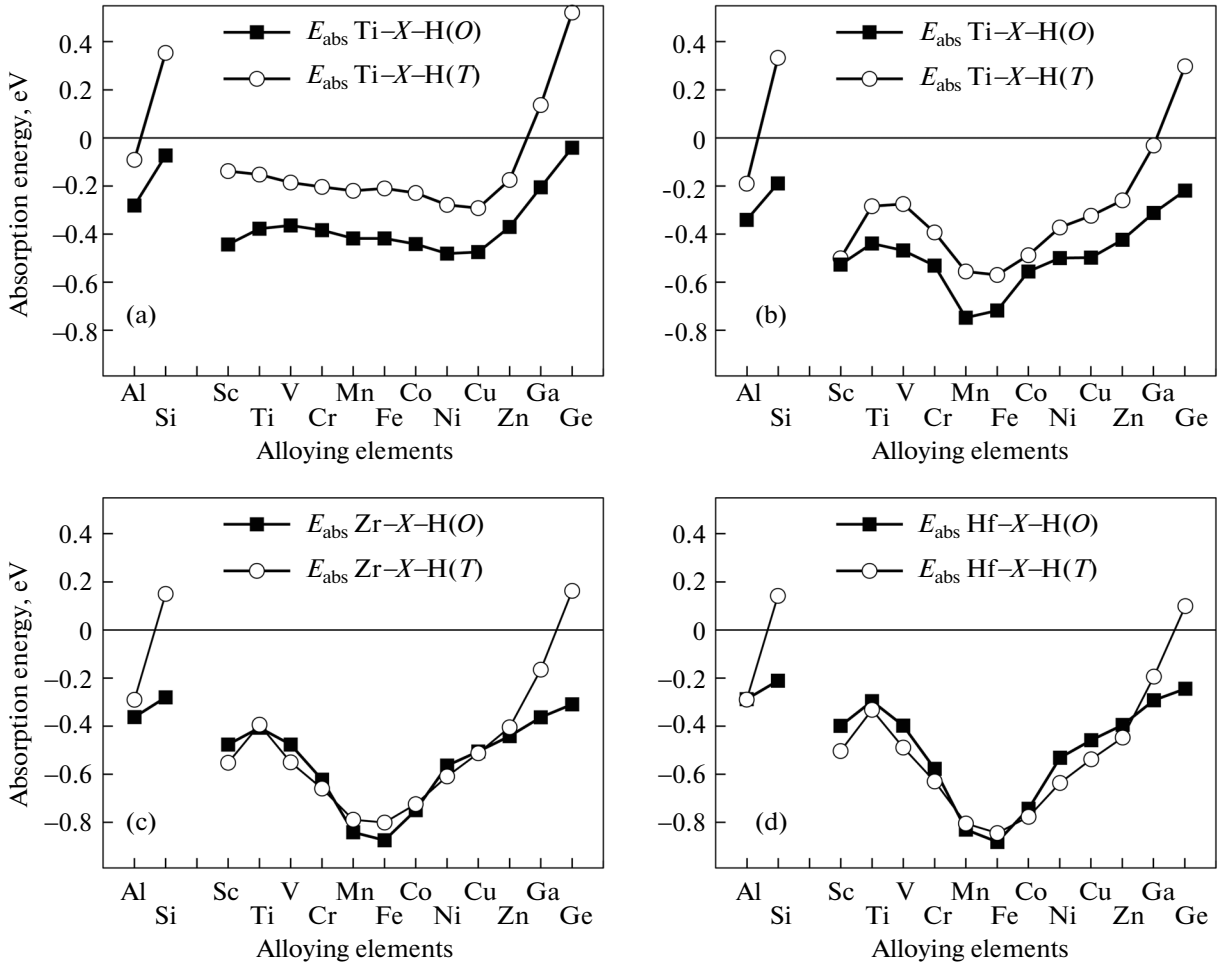

Fig. 3. Influence of impurities on the absorption energy of hydrogen in the octahedral and tetrahedral positions in Group IVB metals, namely, in (a) titanium after the relaxation of the cell volume and (b) titanium, (c) zirconium, and (d) hafnium after the optimization of atomic positions and the relaxation of the cell volume.

d states of the metals with the *s* orbitals of hydrogen. Since an additional electron appears in the system, the electron densities of states are shifted deeper under the Fermi level E_F, which leads to an increase in the number of electron states at the Fermi level E_F.

3.2. Influence of Impurities on the Hydrogen Sorption in Metals

The dependences of the absorption energy of hydrogen in metals for both positions on the type of substitutional impurity are shown in Fig. 3. As in [14], substitutional impurities in our case were 3*d* transition metals and simple metals, such as Al, Si, Ga, and Ge. Recall that the more negative absorption energies mean a better solubility of hydrogen in the material. It can be seen that the obtained curves strongly depend on the method used for optimizing the lattice. The absorption energy of hydrogen in the octahedral positions of titanium is greater in magnitude than that in the tetrahedral positions. This tendency is retained for all the aforementioned impurities. After the optimization of only the titanium cell volume (Fig. 3a), the maximum absorption energies correspond to elements of the end of the 3*d* period (Ni, Cu). However, this tendency changes after the relaxation of atomic positions (Fig. 3b). In this case, the maximum hydrogen sorption energies are observed in titanium alloyed with elements of the middle of the 3*d* period (Mn, Fe). Similar tendencies were also revealed in the case of zirconium and hafnium. Since the hydrogen sorption energies in the considered positions of these metals are approximately equal to each other, the impurities significantly affect the preferred hydrogen sorption positions. As can be seen from Figs. 3c and 3d, impurities of simple metals decrease the absolute value of the hydrogen sorption energy in the *T* positions of the metals, whereas for manganese and iron impurities, the absorption in the *O* positions becomes more preferable as compared to the *T* positions.

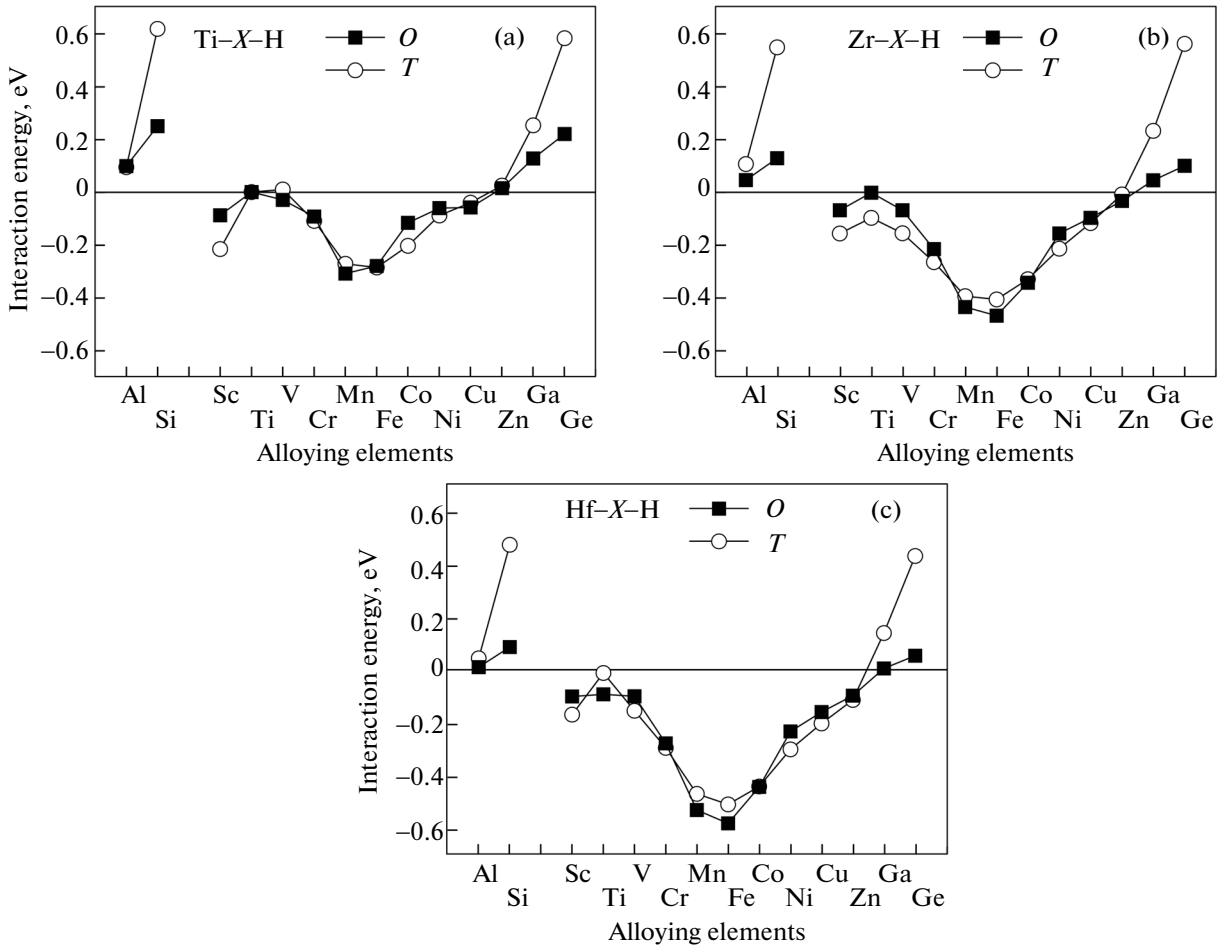

Fig. 4. Interaction energy between an impurity atom and a hydrogen atom in the octahedral and tetrahedral positions in (a) titanium, (b) zirconium, and (c) hafnium.

3.3. Interaction Energy of the Impurity with Hydrogen

Let us now discuss the results of calculations of the interaction energy between hydrogen and impurity atoms in the metal matrix. It can be seen from Fig. 4 that, for all Group IV metals alloyed with simple metals, the interaction energy takes on positive values, regardless of the hydrogen sorption position. This indicates the repulsion between the hydrogen atoms and the atoms of simple metals. In the case of alloying with transition metals, the interaction energy of the impurity with hydrogen is predominantly negative for both positions of the hydrogen atom in the matrix, and the minimum of the curve also corresponds to the middle of the 3*d* period. The negative interaction energy suggests that transition metals attract hydrogen in both the octahedral and tetrahedral positions. At the same time, in [14], the negative interaction energies were obtained only for hydrogen in the tetrahedral positions, except for scandium and zinc, whereas the positive values of ΔE (except for scandium) corresponded to hydrogen in the octahedral positions. It should be noted that, in [14], the dependences of the hydrogen–impurity interaction energy in titanium had the form of a parabola for the *T* positions and an inverse parabola for the *O* positions. In our case, the corresponding dependence, most likely, has a *V*-shaped form, as in [42], where the author considered the influence of impurities on the oxygen sorption in titanium.

In [16, 21], it was suggested that one of the reasons for the trapping of hydrogen by impurity atoms is the difference in the sizes of the impurity atom and the matrix atom. If the size of the impurity atoms is smaller than that of the matrix atoms, the crystal is subjected to stresses and, according to the Matsumoto theory [21], hydrogen tends to occupy sites so as to decrease the stress fields. Meanwhile, if the impurity atoms have large sizes, the interstitial sites nearest to the impurities also become larger in size, which is favorable for hydrogen sorption. It is known that the hydrogen sorption energy increases in the positions located close to vacancies or at the grain boundaries where there is a more space for hydrogen than in the metal matrix [19, 43]. The incorporation of impurity atoms or hydrogen into the crystal structure of the

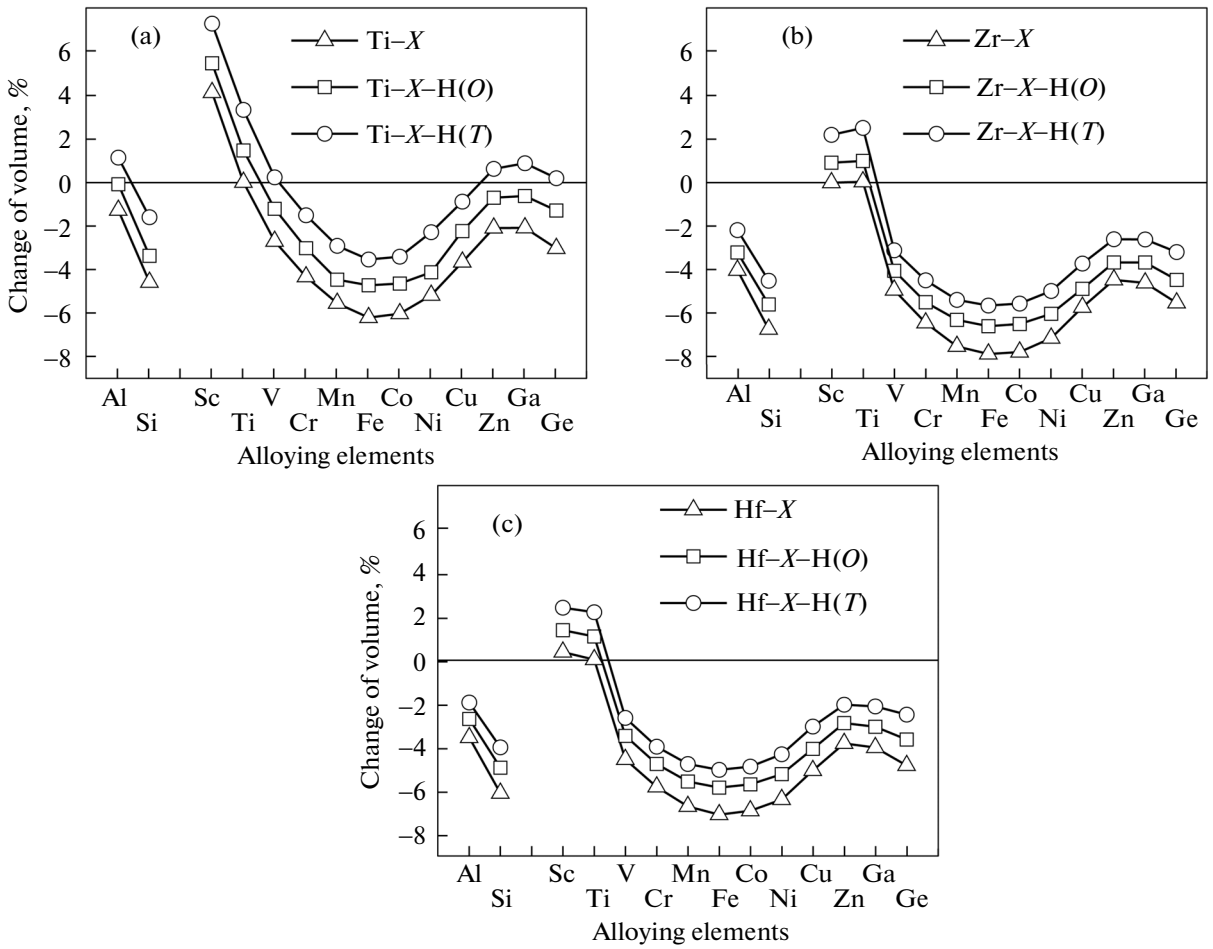

Fig. 5. Relative change in the cell volume of the alloyed metals as a function of the hydrogen position.

metals causes its deformation and leads to a change in the cell volume (Fig. 5). In particular, the incorporation of hydrogen into the metal lattice favors its expansion, and the effect exerted on the change in the volume of the lattice by different alloying impurities is determined by the ratio of their size to the size of the matrix atoms. Consequently, when the cell simultaneously contains a hydrogen atom and an impurity atom with the size smaller than the size of the matrix atom, the internal stress fields are partially compensated. It can also be seen from Fig. 5 that the lattice volume changes more significantly in the case of the hydrogen sorption in the T position. Therefore, according to the Matsumoto theory [21], hydrogen should prefer the T position in the case of impurities with the size smaller than the size of the matrix atom, but, on the other hand, hydrogen is easily embedded in the O position, where the interstitial site has a larger size. In hexagonal close-packed (hcp) metals, the volume of tetrahedra is two times smaller than that of the octahedra. The maximum change in the lattice volume is caused by chemical elements of the middle of the 3*d* period, which correlates with the results of the calculation of the interaction energy of hydrogen with the impurity. This behavior is consistent with that observed previously in [14] for hydrogen in the T position and can be explained in terms of the model proposed in [21]. At the same time, large changes in the volume are also observed in the case of simple metals, which is in disagreement with the energies of their interaction with hydrogen.

3.4. Influence of Hydrogen and Impurities on the Electronic Structure of Metals

Using zirconium as an example, we consider the change in the electronic structure of metals due to alloying and/or hydrogen sorption. The total densities of states of pure zirconium, transition metal impurities, and impurities of simple metals are shown in Fig. 6. It can be seen that the alloying with impurities of transition metals, which have a valence higher than the valence of titanium, leads to a decrease in the number of unoccupied states and to an increase in the number of bonding states below the Fermi level, which is caused by the filling of the *d* band of the metals in the

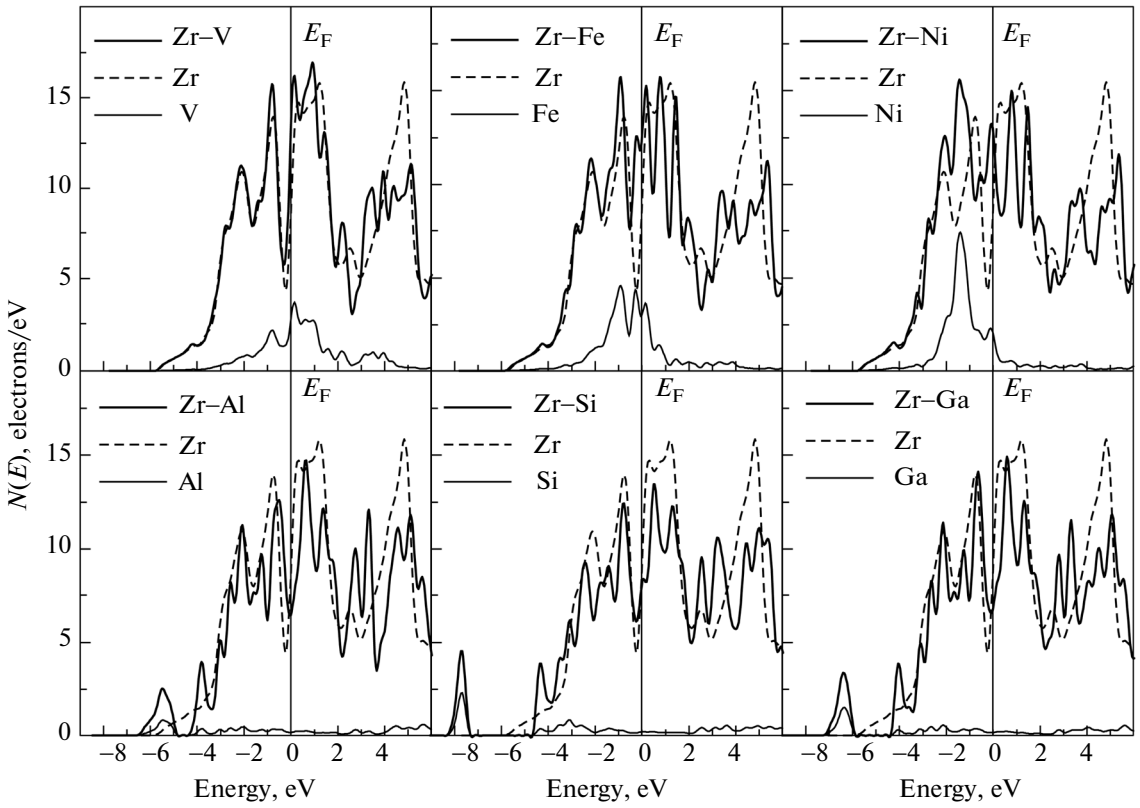

Fig. 6. Influence of impurities on the total densities of states of zirconium. The solid and dashed lines show the densities of states of the alloyed zirconium and pure zirconium, respectively. The thin solid lines indicate the local densities of states of the impurities.

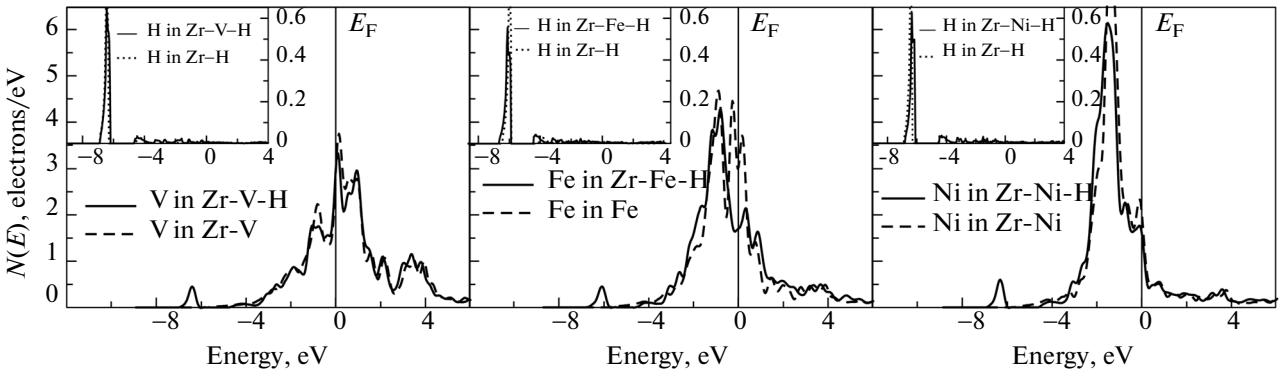

Fig. 7. Local densities of states of the transition metal impurities and hydrogen (in the insets) for the systems Zr–X–H (solid lines) and Zr–X (dashed lines). Hydrogen is in the T position.

series V–Fe–Ni. Although the contribution from simple metals to the total density of states of Group IVB metals is significantly less than the corresponding contribution from 3*d* metals, the observed change in the total density of states in this case is more pronounced. The appearance of small peaks below the bottom of the valence band of zirconium is mainly caused by the states of simple metals. Similar peaks were observed in metals with hydrogen (Fig. 2). At the same time, a simple metal containing only the *s* and *p* states cannot compensate the loss of the contributions from the *d* states to the electron density of states due to the replacement of one of the zirconium atoms by this metal. Recall that the structure of the density of states of transition metals is predominantly formed by the *d* states.

Figure 7 shows the local electron densities of states of transition metals and hydrogen in the Zr–X–H and

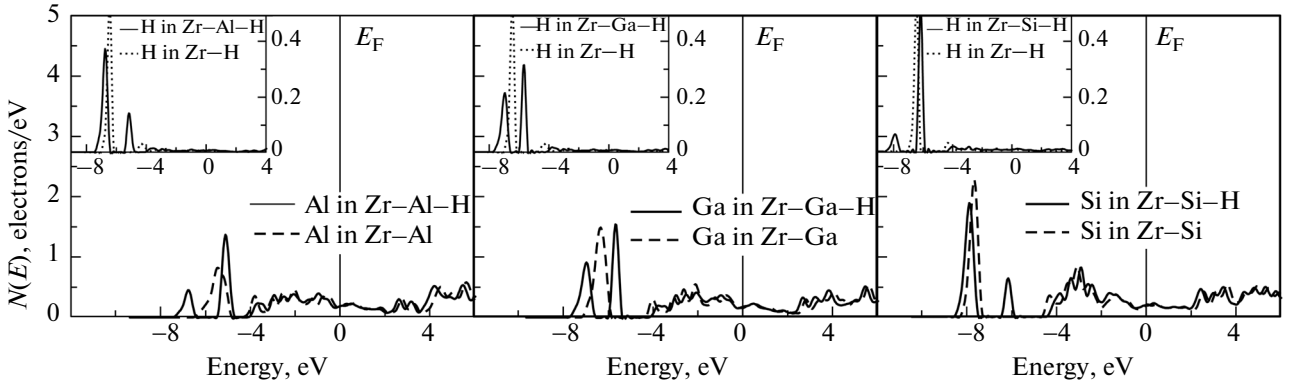

Fig. 8. Local densities of states of the simple metal impurities and hydrogen (in the insets) for the systems Zr–*X*–H (solid lines) and Zr–*X* (dashed lines). Hydrogen is in the *T* position.

Zr–*X* systems, where hydrogen atoms occupy the *T* positions. It can be seen that there are small peaks induced by the hydrogen–impurity interaction, which are located in the energy range from –7.0 to –6.0 eV, where there is the valence band of hydrogen (insets in Fig. 7). Moreover, there is a small shift of the valence states of the metal toward the negative energies due to the interaction of the impurity with the hydrogen *s* states, which leads to an increase in the electron density of states at the Fermi level E_F. It can also be seen from Fig. 7 that the impurity has a weaker effect on the position of the valence band of hydrogen (insets in Fig. 7), because the hybridization between the orbitals of hydrogen and the impurity in this case is similar to the hybridization of the hydrogen and zirconium states. The above tendency is also observed in the case of titanium and hafnium. The results of our calculations for titanium are in good agreement with the results obtained in [14] using the linear muffin-tin orbital atomic-sphere approximation (LMTO–PAS) method. The results presented in Figs. 6 and 7 allow us to conclude that the change in the electronic structure of the *Me*–*X* and *Me*–*X*–H systems is less pronounced upon alloying with transition metals. In this regard, the results obtained for zirconium and hafnium confirm that the electronic factor is not decisive for the explanation of the trapping of hydrogen by an impurity transition metal atom, as was noted in [14] based on the calculations of the Ti–H system.

A somewhat different situation occurs with simple metals. The local electron densities of states of simple metals and hydrogen in the Zr–*X* and Zr–*X*–H systems are shown in Fig. 8. It can be seen that the hybridization of the *s* and *p* orbitals of a simple metal with the hydrogen *s* orbitals leads to a splitting of the low-lying states. These states have predominantly the *s* character, whereas the states lying above –4.0 eV are mainly the *p* states, which follows from the calculations of the partial densities of states. Since the structure of the electronic states of simple and transition metals has been discussed many times in the literature, we do not present their partial densities of states. It should be noted that the *s* and *p* states of simple metals are shifted in opposite directions due to the interaction with hydrogen. As can be seen from Fig. 8, the states of a simple metal in the Zr–*X* systems with Al and Ga lie higher than the hydrogen states in the Zr–H system. Consequently, the hybridization leads to the appearance of a split peak in the density-of-states curves, one component of which is shifted toward lower energies, where there is a peak of hydrogen in pure zirconium. In the case of Si and Ge (the latter is not shown in Fig. 8), their states are located slightly lower than those of hydrogen. Hence, upon hybridization, the density-of-states curves of the metal contain an additional peak due to the interaction with hydrogen, whereas the density-of-states curves of hydrogen exhibit a new small peak shifted toward negative energies. In general, this behavior of the states of hydrogen and a simple metal almost does not depend on the hydrogen sorption position. The hydrogen states located above –4.5 eV are hybridized with the *p* states of the simple metal. It is assumed that hybridization of the hydrogen states with the impurity leads to the formation of both the bonding and antibonding states. In the case of hydrogen, these states are occupied and lie below the Fermi level. The increase in the energy of the system, which is induced by the antibonding states, is greater than the decrease in the energy due to the bonding states, which actually leads to the repulsion of hydrogen and impurity atoms of simple metals. This problem was discussed in more detail in [14]. Thus, the changes in the electronic structure of Group IVB metals upon alloying and incorporation of hydrogen have the same tendencies, and the determining factor of the hydrogen–impurity interaction in the case of simple metals is the electronic factor. Despite the large lattice distortions due to the alloying with simple metals (Fig. 5), the interaction energy of hydrogen with the impurity has positive values, which is inconsistent with the Matsumoto model [21].

4. CONCLUSIONS

In this work, we calculated the binding and absorption energies of hydrogen in Group IVB metals, as well as the hydrogen–impurity interaction energy, where the impurity was considered to be a 3*d*-transition or simple metal. It was shown that hydrogen atoms prefer to occupy octahedral positions in titanium and tetrahedral positions in hafnium, whereas in zirconium, the binding energies of hydrogen in both positions are approximately equal to each other. The difference in the binding energies depends significantly on the procedure used for the optimization of the computational cell. The preference of octahedral positions for hydrogen sorption in titanium is associated with the structural factors. As the structural parameters increase in the series of the metals under consideration, the hydrogen sorption becomes energetically more favorable in tetrahedral positions due to the dominant chemical contribution to the energetics of hydrogen bonding. The mechanical contribution to the energetics of hydrogen bonding with Group IVB metals is small and does not exceed ~0.1 eV. The impurities have no effect on the preferred hydrogen sorption positions in titanium, but their influence is more significant in zirconium and hafnium. The solubility of hydrogen in these metals increases for transition metals in the middle of the 3*d* period. It was found that, irrespective of the sorption position, the interaction energy of hydrogen with transition metal impurities is predominantly negative, whereas the interaction energy of hydrogen with impurities of simple metals is positive; i.e., transition metals attract hydrogen, while simple metals repel it. The interactions of hydrogen with impurities of 3*d*-transition and simple metals are determined by different factors. In the first case, the size effect is dominant and this interaction can be described by the model of relaxation of stress fields, whereas in the second case, the electronic factor dominates.

ACKNOWLEDGMENTS

The study was performed within the framework of the Project No. III.23.1.1 of the Institute of Strength Physics and Materials Science of the Siberian Branch of the Russian Academy of Sciences (Tomsk, Russia) and contains the results obtained during the implementation of the Project No. 8.1.02.2015 within the framework of the Program "D.I. Mendeleev Scientific Foundation of the Tomsk State University."

The numerical calculations were performed on the SKIF-Cyberia supercomputer installed in the Tomsk Regional Center for Collective Use of High-Performance Computing Resources at the National Research Tomsk State University (Tomsk, Russia).

REFERENCES

1. N. E. Paton and J. C. Williams, *Hydrogen in Metals*, Ed. by I. M. Bernstein and A. W. Thompson (American Society for Metals, Metals Park, Ohio, United States, 1974).
2. *Hydrogen in Metals*, Ed. by G. Alefeld and J. Volkl (Springer-Verlag, Heidelberg, 1978; Mir, Moscow, 1981), Vol. 1.
3. K. M. Mackay, *Hydrogen Compounds of the Metallic Elements* (E. and F. N. Spon, London, 1966).
4. V. L. Moruzzi, J. F. Janak, and A. R. Williams, *Calculated Electronic Properties of Metals* (Pergamon, New York, 1978).
5. O. Jepsen, Phys Rev. B: Solid State **12**, 2988 (1975).
6. T. Asada and K. Terakura, J. Phys. F: Met. Phys. **12**, 1387 (1982).
7. P. Blaha, K. Schwarz, and P. H. Dederichs, Phys. Rev. B: Condens. Matter **38**, 9368 (1988).
8. I. Bakonyi, H. Ebert, and A. I. Liechtenstein, Phys. Rev. B: Condens. Matter **48**, 11 (1993).
9. D. A. Papaconstantopoulos and A. C. Switendick, J. Less-Common. Met. **103**, 317 (1984).
10. M. Gupta, Solid State Commun. **29**, 47 (1979).
11. S. E. Kul'kova, O. N. Muryzhnikova, and I. I. Naumov, Phys. Solid State **41** (11), 1763 (1999).
12. C. Domain, R. Besson, and A. Legris, Acta Mater. **50**, 3513 (2002).
13. D. Connetable, J. Huez, E. Andrieu, and C. Mijoule, J. Phys.: Condens. Matter **23**, 405401 (2011).
14. Q. M. Hu, D. S. Xu, R. Yang, and D. Li, Phys. Rev. B: Condens. Matter **66**, 064201 (2002).
15. X. L. Han, Q. Wang, D. L. Sun, T. Sun, and Q. Guo, Int. J. Hydrogen Energy **34**, 3983 (2009).
16. J. F. Miller and D. G. Westlake, Trans. Jpn. Inst. Met. **21** (Suppl.), 153 (1980).
17. C. Korn and D. Teitel, Phys. Status Solidi A **44**, 755 (1977).
18. H. Chou and T. J. Rowland, Phys. Rev. B: Condens. Matter **45**, 11 590 (1992).
19. Y. J. Li, S. E. Kulkova, Q. M. Hu, D. I. Bazhanov, D. S. Xu, Y. L. Hao, and R. Yang, Phys. Rev. B: Condens. Matter **76**, 064110 (2007).
20. G. Lee, J. S. Kim, Y. M. Koo, and S. E. Kulkova, Int. J. Hydrogen Energy **27**, 403 (2002).
21. T. Matsumoto, J. Phys. Soc. Jpn. **42**, 1583 (1977).
22. H. L. Skriver, *The LMTO Method* (Springer-Verlag, Berlin, 1983).
23. R. Hempelmann, D. Richter, and B. Stritzker, J. Phys. F: Met. Phys. **12**, 79 (1982).
24. R. Khoda-Bakhsh and D. K. Ross, J. Phys. F: Met. Phys. **12**, 15 (1982).
25. R. Griessen, Phys. Rev. B: Condens. Matter **38**, 3690 (1988).
26. Q. Xu and A. Van der Ven, Phys. Rev. B: Condens. Matter **76**, 064207 (2007).
27. M. H. Kang and J. W. Wilkins, Phys. Rev. B: Condens. Matter **41**, 10182 (1990).
28. P.E. Blöchl, Phys. Rev. B: Condens. Matter **50**, 17953 (1994).

29. G. Kresse and J. Joubert, Phys. Rev. B: Condens. Matter **59**, 1758 (1999).
30. G. P. Kresse and J. Hafner, Phys. Rev. B: Condens. Matter **49**, 14 251 (1994).
31. G. Kresse and J. Furthmüller, Comput. Mater. Sci. **6**, 15 (1996).
32. J. P. Perdew, K. Burke, and M. Ernzerhof, Phys. Rev. Lett. **77**, 3865 (1996).
33. H. J. Monkhorst and J. D. Pack, Phys. Rev. B: Solid State **13**, 5188 (1976).
34. N. Ashcroft and N. Mermin, *Solid State Physics* (Holt, Rinehart and Winston, New York, 1976; Mir, Moscow, 1979).
35. S. S. Pan, M. L. Yeater, and M. E. Moore, Trans. Am. Nucl. Soc. **9**, 495 (1966).
36. W. Drexel, A. Murani, D. Tocchetti, W. Kley, J. Sosnowka, and D. K. Ross, J. Phys. Chem. Solids **37**, 1135 (1976).
37. R. Caputo and A. Alavi, Mol. Phys. **101**, 1781 (2003).
38. O. V. Lopatina, Yu. M. Koroteev, and I. P. Chernov, Phys. Solid State **56** (5), 1009 (2014).
39. http://www.flapw.de.
40. Yu. M. Koroteev, O. V. Lopatina, and I. P. Chernov, Izv. Vyssh. Uchebn. Zaved., Fiz. **55**, 276 (2012).
41. A. Y. Lozovoi and A. T. Paxton, Phys. Rev. B: Condens. Matter **77**, 165 413 (2008).
42. H. Wu, PhD Thesis (University of Illinois, Urbana, Illinois, United States, 2013).
43. S. E. Kulkova, A. V. Bakulin, S. S. Kulkov, S. Hocker, and S. Schmauder, J. Exp. Theor. Phys. **115** (3), 462 (2012).

Translated by O. Borovik-Romanova